A Numerical Analysis on the Shedding Mechanism of Dripping Flame

Xinyan Huang[1], Caiyi Xiong[2], Peiyi Sun[1], Yong Jiang[2]

[1]Research Center for Fire Engineering, The Hong Kong Polytechnic Univerisity
Kowloon, Hong Kong
[2]State Key Laboratory of Fire Science, Univerisity of Science and Technology of China
Hefei, Anhui, China

1 Introduction

The dripping of molten fuel is a phenomenon that occurs frequently in fire [1]. The most common case of dripping is the burning candle [2] (Fig. 1a), where the molten wax flows downward by gravity and forms a drip without the flame attachment. In contrast to the dripping phenomenon in candle flame, the drips from thermo-plastic materials can often carry flames, such as those in façade fires (Fig. 1b) and electrical wire fires (Fig. 1c). Drips with flame can ignite nearby combustibles, promote the fire spread, cause explosions and enlarge the dangerous scope of fire [3–8]. As such, research on the dynamics of dripping flame is of both scientific interest and practical importance.

The dripping flame is essentially a drip of hot liquid fuel surrounded by the flame that is sustained by pyrolysis gases. In our previous work [1], drips with diameter of 2~3 mm and flame attachment was generated from the burning polyethylene (PE) wire. The duration of semi-free fall for a height of 2.6 m was less than 1.0 s. Interesting, the dripping flame appeared to be a blue chain of flame visually as a result of persistence vision (Fig. 1d). By the use of high-speed camera, the dripping flame was shown to be a "flame-shedding" process (Fig. 1e) which has a similar shedding frequency to the von Karman vortex. The sound analysis further suggested that the flame shedding was a continuous ignition of flammable mixture behind the drip, i.e., continuous small explosions (Fig. 1e).

Due to the fast motion and the tiny size of the falling drip, there can be large uncertainties and difficulties in exploring the dripping flame dynamics, e.g. temperature and vorticity fields of drip and flame shedding, via experimental techniques. Comparatively, numerical simulation is more useful to gain further insights on the dripping problem by simplifying physical problem and controlling the parameters. However, it is a computational challenge because the process of accelerating dripping and flame shedding is transient and different from a porous spherical gas burner in a constant flow [9, 10]. It is suspected that the acceleration

Correspondence to: ycxiong@mail.ustc.edu.cn

of drip by gravity not only plays an important role in the flame shedding from the drip, but may also be responsible for the flame extinction during the falling. To authors' best knowledge, very few literatures have simulated the dripping flame or the flame-shedding process, so there is a knowledge gap.

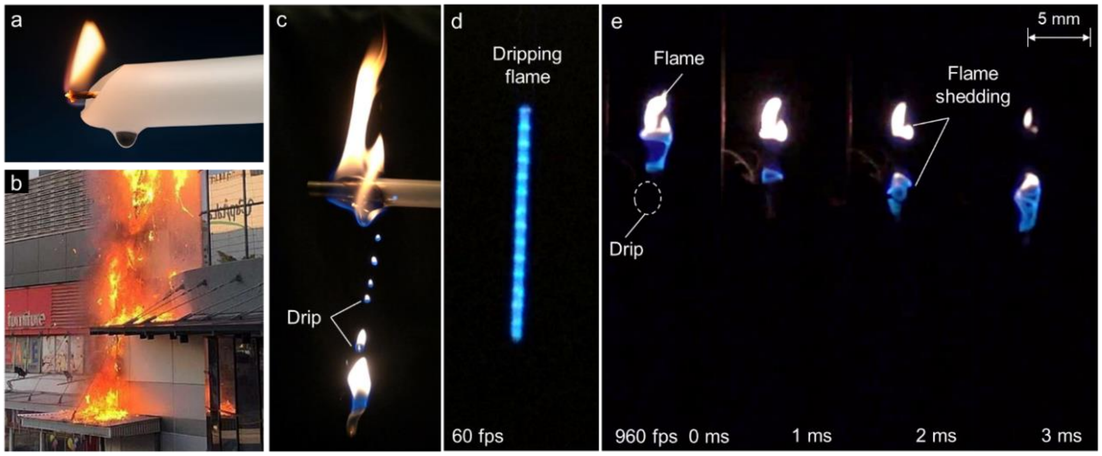

Figure 1. (a) Drip from a candle flame, (b) dripping fire spread in façade, (c) drips from a research wire, and snapshot of dripping flame by (d) a regular camera at 60 fps, and (e) a high-speed camera at 960 fps.

The aim of this paper is to develop a simplified model to demonstrate the vortex mechanism of dripping flame by Direct Numerical Simulation (DNS). A parametric study by varying the acceleration of flame during falling is carried out to show the evolution of flame shedding. Moreover, a vorticity transport equation is employed to examine the transport budgets leading to the formation and evolvement of the vortex shedding phenomenon.

2 Numerical Model

In the present work, the Fire Dynamic Simulator (FDS 6.6) with DNS solver [11] is used to construct the numerical model. As a logical first step, a simplified 2-D computational box is used to simulate both the falling drip and the following tiny explosion. A planar Cartesian coordinate (x, y) is utilized to show the geometric position, where x stands for the horizontal direction and y denotes the vertical direction. The convergence study suggested a uniform grid with 120 nodes in the horizontal direction from x = -1.2 cm to 1.2 cm and 350 nodes in the vertical direction from y = -1 cm to 6 cm, providing a mesh resolution of Δl = 0.2 mm (refer to Fig. 2). A collapsing sphered drip with the diameter of 2 mm is placed inside the computational domain, where its center coincides with the origin of the coordinate system. This geometric configuration is the same as that used in our previous work for studying the non-reactive vortex shedding from drip [1]. The upgrade in this work lies in that the flame chemistry in the gas-phase is further considered to simulate the actual flame shedding process in Fig. 1(e).

The whole box is bounded by four boundaries, including the bottom inflow boundary and the open boundary condition for the top and two side boundaries (refer to Fig. 2). To simplify the problem, the physical problem investigated in the first step is that a single burning drip falling to the ground at a constant velocity without acceleration. Therefore, the position of drip is fixed, and a constant upward flow field is set by the inflow boundary to mimic the falling process of constant velocity (U_a). The dripping flame is described by the 1-step finite rate gas kinetics [12]. To simplify the process, the condensed-phase pyrolysis reaction is not considered. Instead, we assume the drip to release the hot ethylene gas of 400 ℃ (i.e., the pyrolysis point of PE) at a mass flux of 0.01 kg/m^2-s (i.e., a Stefan flow). Additional fuel is injected on the top half surface of drip at a prescribed velocity (V_f). There are two reasons for setting the fuel jet: (1) to partially mimic the acceleration of drip, because in the coordinate of accelerating drip, the fuel in the recirculation zone seems to have an initial velocity; and (2) the flame shedding is similar to lifted jet flames (see Fig. 1e). Different fuel jet velocities are examined to investigate the critical condition for flame shedding and extinction.

To imitate a flame, a hot igniter with a peak temperature of 1400 ℃ is placed in a single mesh that is 1 cm above the center of spherical drip. The piloted ignition process lasts for 0.7 s without imposing the airflow, which is sufficient to produce a stable flame. Afterward, the heat source will be removed, and the upward flow is imposed and increased linearly to V_a within 1 s. The whole computational domain is set to have an ambient temperature and pressure of 25 ℃ and 1atm, respectively. The simulation time advances evenly at a short step of 1 ms for chemical restraint. The computation was implemented on ThinkServer RD640 (Xeon, 2.1 GHz) with 13 threads. For modelling the process of 8 s, each model required approximately 10 days of CPU time.

3 Results

Referring to our previous experiments [1], a drip with the diameter of 2mm (D) is simulated under a fixed airflow velocity of V_a = 3 m/s (Re = $V_a D/\nu \approx 400$), which is smaller than its free-fall terminal velocity of about 4 m/s. The base case, without fuel jet (V_f = 0 m/s) and a pure Stefan flow (0.01 kg/m^2-s) for the entire sphere, is first simulated with and without the flame chemistry. Figure 2(a) show the temperature contour (℃) without the flame chemistry (i.e., non-reactive) after the flow is stabilized. As expected, a classical von Karman vortex street is observed under a shedding frequency of 615 Hz. Figure 2(b) shows the base case with 1-step flame chemistry and its contour of heat release rate (kW/m^3) and temperature (℃) after the flame is ignited and stabilized. In contrast, the flame shedding does not occur. Instead, a stable diffusion flame is observed, and it essentially simulates the experiment of a porous spherical gas burner in a constant flow [9, 10]. Further increasing the airflow velocity, the flaming shedding still does not occur before the blow off.

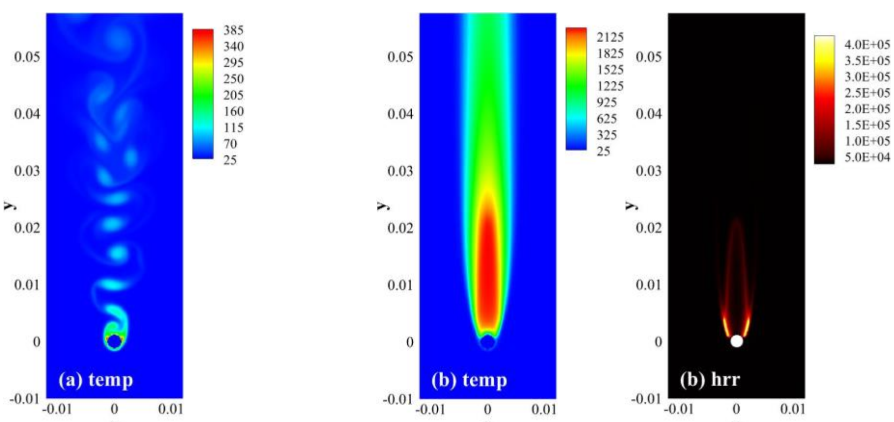

Figure 2. Base case of the pure Stefan flow with a fuel mass flux of 0.01 kg/m2-s, (a) without flame chemistry (non-reactive flow), and (b) with 1-step flame chemistry, where drip diameter is 2 mm, and the air flow is 3 m/s.

Then, the dripping flame was simulated over a wide range of fuel jet velocities (V_f = 0.2 ~ 0.5 m/s), as shown in Fig. 3. Note that flame acceleration behaves as a step-like ascent from left to right with an increment of 0.1 m/s. Their instantaneous contours of the heat release rate are used to indicate the shape of dripping flame when the flame is fully developed. For the lowest fuel jet velocity (V_f = 0.2 m/s) in Fig. 3(a), the flow field is very laminar and similar to the base case in Fig. 2(b), like a classical Burke-Schumann diffusion flame. Because of the low fuel-jet velocity, the flame still covers the drip, and the lift-flame structure is not observed.

Increasing the jet velocity to 0.3 m/s in Fig. 3(b), the prominent feature for the dripping with faster flame shedding starts to occur, where the development of vortex street behind the drip only occurs in the right-hand side. It also implies that V_f = 0.3 m/s is near the critical condition for triggering the flame shedding.

At V_f = 0.4 m/s, a symmetric and stable flame shedding is found, and the enhanced vortex structure can be observed with fluctuations propagating in the upward direction. At V_f = 0.5 m/s, the flame shedding become asymmetric, and more importantly, it shows a reasonable similarity to experimental snapshots in Fig. 1(e), where a stronger flamelet is sitting above a weak flamelet. Moreover, as expected for the lifted jet flame, the distance between the top hemi-sphere and the flame base is in a positive correlation to the fuel jet velocity. This further suggests that (i) flame acceleration is indeed a factor that causes the flame shedding, and (ii) the structure of flame shedding behind the drip is similar to the lifted jet flame. Considering the simplicity of the proposed model, it is a good step forward to reproduce the real flaming shedding of a PE drip.

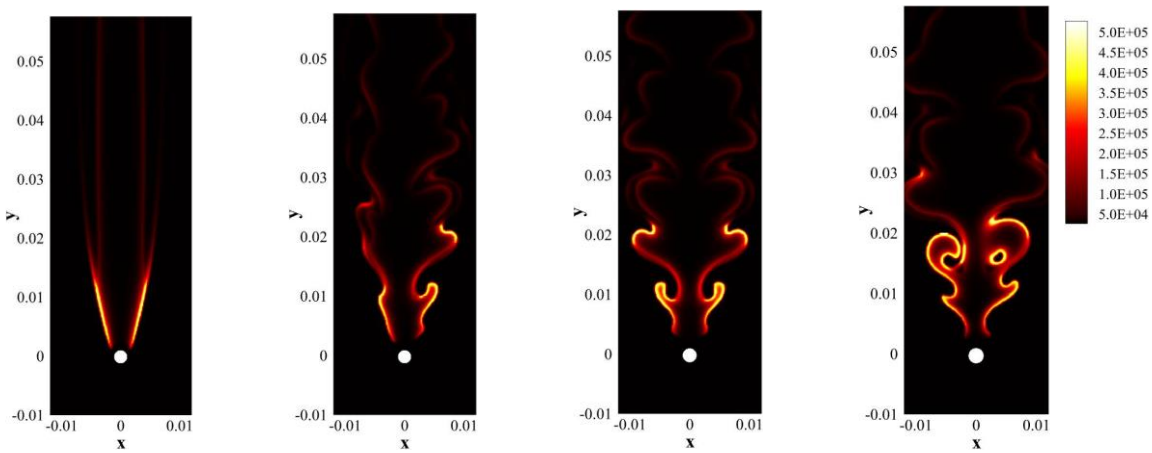

(a) V_f = 0.2 m/s (b) V_f = 0.3 m/s (c) V_f = 0.4 m/s (d) V_f = 0.5 m/s

Figure 3. Instantaneous surfaces of heat release rate (kW/m^3) for the cases with fuel jet velocity (V_f) of (a) 0.2 m/s, (b) 0.3 m/s, (c) 0.4 m/s and (d) 0.5 m/s, where drip diameter is 2 mm, and the air flow is 3 m/s.

To further explore the relation between flame acceleration and the vortex field, a planar vorticity transport equation [13] is utilized,

$$\frac{D\omega}{Dt} = -\omega\left(\frac{\partial u}{\partial x}+\frac{\partial v}{\partial y}\right)+\frac{1}{\rho^2}\left(\frac{\partial \rho}{\partial x}\frac{\partial p}{\partial y}-\frac{\partial \rho}{\partial y}\frac{\partial p}{\partial x}\right)+\frac{\mu}{Re}\left(\frac{\partial^2\omega}{\partial x^2}+\frac{\partial^2\omega}{\partial y^2}\right)-\frac{1}{\rho^2}\frac{\rho_a g}{Fr}\frac{\partial \rho}{\partial y} \tag{1}$$

where $D/Dt = \partial/\partial t + u_i\partial/\partial x_i$ is the convection derivative, ω is the vorticity, t is time, p is the pressure, ρ is the density, u and v are the velocities in horizontal and vertical directions, μ is the viscosity, Re is the Reynolds number and Fr is the Froude number. Parameters used to nondimensionalize the model include the drip diameter D, the characteristic velocity $V = \sqrt{2gD}$ and the gas parameters of air at room pressure and temperature. Terms on the right-hand side of Eq. (1) are volumetric expansion, baroclinic torque due to the misalign between pressure gradient and density gradient, viscous term and gravitational term.

The non-dimensional distributions of vorticity for each case are shown in Fig. 4. It is worth to note that in a 2-D planar space, only the vorticity $\omega = \partial v/\partial x - \partial u/\partial y$ which is perpendicular to the plane is nonzero. The first striking observation in Fig. 4 is that the positive vortices are pronounced in the right part of domain, whereas the negative vortices tend to gather in the left domain. This is due to the sign change of horizontal velocity u across the drip centerline x=0. According to Eq. (1), the importance of gravitational term on the initial formation of vorticity can be seen clearly since this term is the only nonzero budget at the beginning of simulation. After the initial stage, all terms will exert impacts on the vorticity transport.

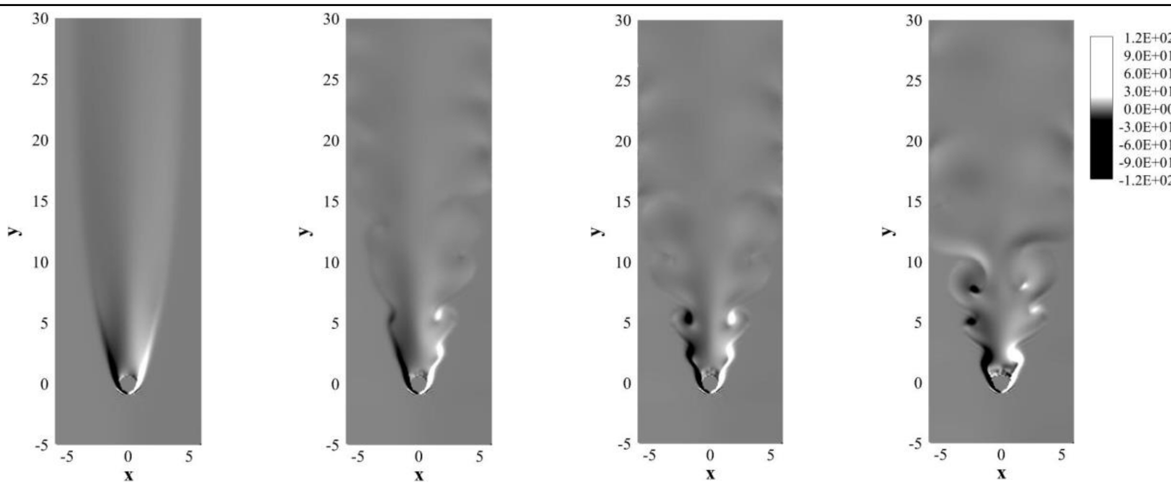

(a) V_f = 0.2 m/s (b) V_f = 0.3 m/s (c) V_f = 0.4 m/s (d) V_f = 0.5 m/s

Figure 4. Contours of non-dimensional vorticity for each case.

We now take the case with V_f = 0.5 m/s as an example to demonstrate the shedding mechanism. Figure 5 shows the snapshots of each transport budget that correspond to the vortical field in Fig. 4(d). The b/w color is used here again to distinguish the positive and negative distributions, where white stands for positive values and black means negative.

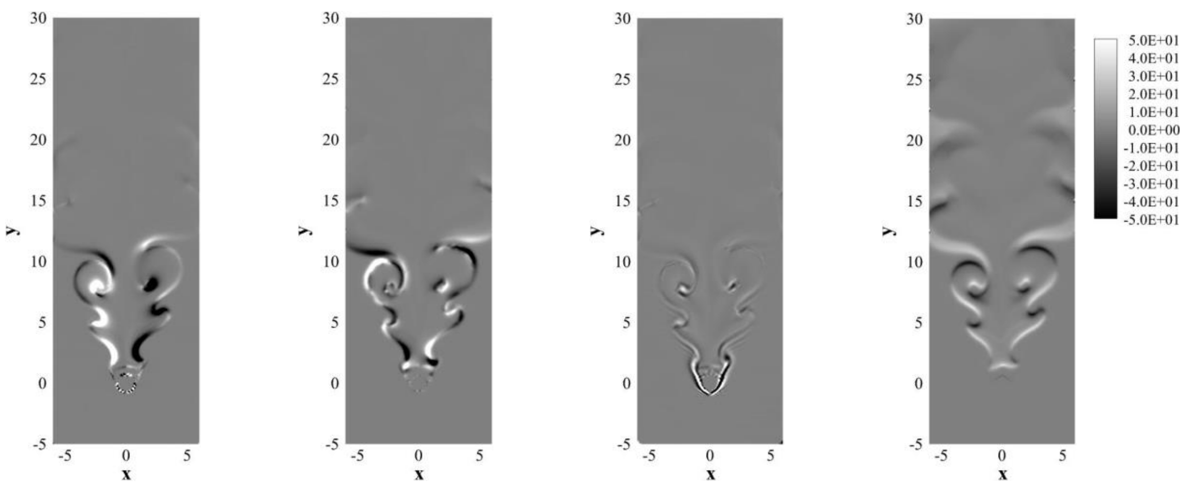

(a) Volumetric expansion (b) Baroclinic torque (c) Viscous term (d) Gravitational term

Figure 5. Contours of the vorticity transport budgets for the dripping with V_f = 0.5 m/s.

It is visible from Fig. 5 that the volumetric expansion is negatively correlated with the vorticity distribution, i.e., the negative expansion term is prevalent on the flame surface where the vorticity is positive, and positive expansion term tends to occur where the vorticity is negative. This indicates that the volumetric expansion of gas leads to an inhibitory effect to the development of vortical structures. Meanwhile, this law applies equally to the viscous term, evidenced by the similar distributions between Figs. 5(a) and 5(c). However, the distribution of viscous term is narrower than volumetric expansion, indicating a less importance of viscosity.

Among all transport budgets, the baroclinic torque behaves as the leading term which dominates the development of vorticity. The comparison between Figs. 5(b) and 4(d) shows that baroclinic torque is positively correlated with the vorticity distribution. As for the gravitational term, however, it only distributes on the outline of flame surface. Furthermore, it can be observed that the gravitational term has both creation and destruction effects on the vorticity, depending on the local flame structure.

Admittedly, the 2-D dripping flames differ from the fully turbulent ones, but the insights obtained from simplified configurations can aid the understanding of shedding mechanism. The critical conditions and extinction mechanism will be discussed more with an upgraded model in our future work.

References

[1] Huang XY. (2018). Critical drip size and blue flame shedding of dripping ignition in fire. Sci. Rep. 8: 16528.

[2] Faraday M. (1885). The chemical history of a candle. Resonance.

[3] Xie QY, Tu R, Wang N, Ma X, Jiang X. (2014). Experimental study on flowing burning behaviors of a pool fire with dripping of melted thermoplastics. J. Hazard. Mater. 267: 48.

[4] Wang Y, Kang WD, Zhang XY, Chen C, Sun PP, Zhang F, Li SX. (2018). Development of a pendant experiment using melt indexer for correlation with the large-size dripping in the UL - 94 test. Fire. Mater. 42: 436.

[5] He H, Zhang QX, Tu R, Zhao LY, Liu J, Zhang YM. (2016). Molten thermoplastic dripping behavior induced by flame spread over wire insulation under overload currents. J. Hazard. Mater. 320: 628.

[6] Miyamoto K, Huang XY, Hashimoto N, Fujita O, Fernandez-Pello C. (2016). Limiting oxygen concentration (LOC) of burning polyethylene insulated wires under external radiation. Fire Saf. J. 86: 32.

[7] Kobayashi Y, Huang XY, Nakaya S, Tsue M, Fernandez-Pello C. (2017). Flame spread over horizontal and vertical wires: The role of dripping and core. Fire Saf. J. 91: 112.

[8] Kobayashi Y, Konno Y, Huang XY, Nakaya S, Tsue M, Hashimoto N, Fujita O, Fernandez-Pello C. (2018). Effect of insulation melting and dripping on opposed flame spread over laboratory simulated electrical wires. Fire Saf. J. 95: 1.

[9] Gollahalli S R, Brzustowski T A. (1973). Experimental studies on the flame structure in the wake of a burning droplet. Symp. (Int.) Combust. 14: 1333.

[10] Raghavan V, Babu V, Sundararajan T, Natarajan R. (2005). Flame shapes and burning rates of spherical fuel particles in a mixed convective environment. Int. J, Heat. Mass Tran. 48: 5354.

[11] McGrattan K, Hostikka S, McDermott R, Floyd J, Weinschenk C, Overholt K. (2013). Fire dynamics simulator technical reference guide volume 1: mathematical model. NIST Spec. Publ. 1018: 175.

[12] Fereres S, Lautenberger C, Fernandez-Pello C, Urban D, Ruff G. (2012). Understanding ambient pressure effects on piloted ignition through numerical modeling. Combust. Flame. 12: 3544.

[13] Jiang X, Luo KH. (2000). Spatial direct numerical simulation of the large vortical structures in forced plumes. Flow, Turbul. Combust. 64: 43.